Available online at www.sciencedirect.com
SCIENCE DIRECT®
International Journal of Solids and Structures 42 (2005) 6181–6201
INTERNATIONAL JOURNAL OF SOLIDS and STRUCTURES
www.elsevier.com/locate/ijsolstr

A theoretical analysis of piezoelectric/composite laminate with larger-amplitude deflection effect, Part II: Hermite differential quadrature method and application

Jinquan Cheng [a,b,*], Biao Wang [a], Shan-Yi Du [a]

[a] Center for Composite Materials, Harbin Institute of Technology, Harbin 150001, PR China
[b] Department of Civil Engineering, Dalhousie University, P.O. Box 1000, Halifax, NS, Canada B3J 2X4

Received 28 April 2004; received in revised form 18 April 2005
Available online 16 June 2005

Abstract

Incorporating the effects of larger-amplitude deflection and electro-elastical properties of piezoelectric lamina, the Hamilton's variation principle was used to deduce the fundamental formulations of smart anisotropic composite plate in Part I in terms of Reddy's simple higher-order theory. In order to solve the five highly coupled nonlinear partial differential equations with complicated overlapping boundary conditions, a novel numerical method-Hermite differential quadrature (HDQ) method was developed to implement the differential equations with complicated overlapping boundary conditions. Based on the presently developed HDQ method, any orders derivatives of the unknown functions or any boundary conditions can be point-collocation-based discretized by a set of point-values along x- and y-direction. Then, a system of complete algebraic nonlinear equations can be constructed to calculate out the final point-values of the mid-plane displacements by using the governing equations and relative boundary conditions with HDQ method. Finally, some detailed numerical examples for the anisotropic piezoelectric/composite laminate with the distributed poling directions of piezoelectric layer and fiber orientations of composite layers were studied to validate the developed theoretical analysis model and HDQ numerical method.

1. Introduction

Increasing uses of the adaptive/intelligent structures and systems integrated with piezoelectric materials as actuators/sensors in the field of engineering have attracted world-wide researchers' attentions. From the

* Corresponding author.
E-mail address: hitcjq@hotmail.com (J. Cheng).

0020-7683/$ - see front matter
doi:10.1016/j.ijsolstr.2005.04.008

viewpoint of design and optimization, it is important and necessary to theoretically predict the static and dynamic electro-mechanical characteristics of composite plate contained piezoelectric layers firstly (Kenji, 1998). Up to now, many researchers had afforded their best to model and investigate the mechanical and electric characteristics of piezoelectric/composite plate so as to reveal the actuating and sensing properties of piezoelectric materials in the smart structures and systems. However, most of these works were based on the classic laminated plate theory or first-order shear deformation theory with the analytical method or the FEM method for some cases (Crawley and Anderson, 1989; Lee, 1990; Pai et al., 1993; Tzou and Zhong, 1993; Donthireddy and Chandrasha, 1996; Zhang and Sun, 1996; Liu et al., 1999; Seeley and Chattopadhyay, 1999; Cheng et al., 2000; Cheng and Batra, 2000; Gopinathan et al., 2000; Wu et al., 2001; Fernandes and Pouget, 2002). On the other hand, with the wider and wider applications of composite structure in the field of engineering, the high accuracy models are demanded for the better understanding of the mechanical properties of composite structure. However, it is a challenge for people to solve the highly coupled governing equations, especially the nonlinear ones, of anisotropic composites. Up to date, only some analytical solutions for the special laminated plates/shells in some special boundary conditions had been successfully worked out by assuming the special Fourier series solution (Hobson, 1926; Whitney and Leissa, 1970; Chaudhuri, 1989). In order to overcome the limitation of the analytical solution, the numerical methods have been widely employed to carry out the final results though their accuracy has been discounted, including the FEM, FDM and point-collocation-based methods etc. Since the point-collocation-based numerical methods can overcome some shortcomings of FEM, such as remeshing and needing more memory etc., they have provoked many researchers' interests. Differential quadrature (DQ) method, as one of the main point-collocation-based numerical methods, has been verified as an effective numerical method to solve the differential equations with boundary conditions (Bellman and Casti, 1971; Villadsen and Michelsen, 1978; Bert and Malik, 1996; Bellomo, 1997; Shu, 2000). But, it is also not easy to implement the overlapping boundary conditions case even though some works had been done by Liu and Wu (2001a,b). Here, it is clearly shown in Part I that the fundamental formulations of anisotropic PZT/composite laminate are five highly coupled nonlinear partial differential equations with complicated overlapping boundary conditions. Therefore in this paper, we based on the famous Hermite interpolation theorem to develop a new generalized differential quadrature method, here called as generalized Hermite differential quadrature (HDQ) method. In the light of the developed generalized HDQ method, the overlapping boundary conditions can be easily implemented as well as the governing equations can be easily discretized by a set of point-values along x- and y-direction. Then, a system of complete algebraic nonlinear equations can be obtained to calculate the scattered point-values of the mid-plane displacements. Furthermore, some electro-elastic properties of anisotropic PZT/composite laminate with the different poling directions and boundary conditions were detailedly analyzed by the presently developed theoretical analysis model and HDQ method.

2. Development of a numerical method: Hermite differential quadrature

From the theoretical analysis of Part I, it is obviously presented that the governing formulations of the smart laminated composite plate presented by the mid-plane displacements are consisted of third-order partial differentiation of u_0, v_0, ϕ_x and ϕ_y and fourth-order partial differentiation of w_0 with respect to x and y as follows:

$$\begin{aligned} &L_{1,1}u_0 + L_{1,2}v_0 + L_{1,3}\phi_x + L_{1,4}\phi_y + L_{1,5}w_0 + q_x - \left(\frac{\partial N_x^P}{\partial x} + \frac{\partial N_{xy}^P}{\partial y}\right) \\ &\quad + \frac{\partial w_0}{\partial x}L_{1,1}w_0 + \frac{\partial w_0}{\partial y}L_{1,2}w_0 = I_0\ddot{u}_0 + \bar{I}_1\ddot{\phi}_x - \frac{4}{3}I_3\frac{\partial^3 w_0}{\partial x\,\partial t^2}, \end{aligned} \tag{1a}$$

$$L_{2,1}u_0 + L_{2,2}v_0 + L_{2,3}\phi_x + L_{2,4}\phi_y + L_{2,5}w_0 + q_y - \left(\frac{\partial N_y^P}{\partial y} + \frac{\partial N_{xy}^P}{\partial x}\right)$$

$$+ \frac{\partial w_0}{\partial x} L_{1,2} w_0 + \frac{\partial w_0}{\partial y} L_{2,2} w_0 = I_0 \ddot{v}_0 + \bar{I}_1 \ddot{\phi}_y - \frac{4}{3} I_3 \frac{\partial^3 w_0}{\partial y \partial t^2}, \tag{1b}$$

$$L_{3,1}u_0 + L_{3,2}v_0 + L_{3,3}\phi_x + L_{3,4}\phi_y + L_{3,5}w_0 + \frac{2}{3}m_x - \left[\frac{\partial M_x^P}{\partial x} + \frac{\partial M_{xy}^P}{\partial y} - Q_x^P + \frac{4}{h^2}S_x^P - \frac{4}{3h^2}\left(\frac{\partial T_x^P}{\partial x} + \frac{\partial T_{xy}^P}{\partial y}\right)\right]$$

$$+ \frac{\partial w_0}{\partial x} L_{1,3} w_0 + \frac{\partial w_0}{\partial y} L_{2,3} w_0 = I_0 \ddot{u}_0 + \bar{I}_2 \ddot{\phi}_x - \frac{4}{3} \bar{I}_3 \frac{\partial^3 w_0}{\partial x \partial t^2}, \tag{1c}$$

$$L_{4,1}u_0 + L_{4,2}v_0 + L_{4,3}\phi_x + L_{4,4}\phi_y + L_{4,5}w_0 + \frac{2}{3}m_y - \left[\frac{\partial M_y^P}{\partial y} + \frac{\partial M_{xy}^P}{\partial x} - Q_y^P + \frac{4}{h^2}S_y^P - \frac{4}{3h^2}\left(\frac{\partial T_y^P}{\partial y} + \frac{\partial T_{xy}^P}{\partial x}\right)\right]$$

$$+ \frac{\partial w_0}{\partial x} L_{1,4} w_0 + \frac{\partial w_0}{\partial y} L_{2,4} w_0 = I_0 \ddot{v}_0 + \bar{I}_2 \ddot{\phi}_y - \frac{4}{3} \bar{I}_4 \frac{\partial^3 w_0}{\partial y \partial t^2}, \tag{1d}$$

$$L_{5,1}u_0 + L_{5,2}v_0 + L_{5,3}\phi_x + L_{5,4}\phi_y + L_{5,5}w_0 - q + \frac{1}{3}\left(\frac{\partial m_x}{\partial x} + \frac{\partial m_y}{\partial y}\right)$$

$$- \left[\frac{\partial Q_x^P}{\partial x} + \frac{\partial Q_y^P}{\partial y} - \frac{4}{3h^2}\left(\frac{\partial^2 T_x^P}{\partial x^2} + \frac{\partial^2 T_{xy}^P}{\partial x \partial y} + \frac{4}{3h^2}\frac{\partial^2 T_y^P}{\partial y^2}\right) + \frac{4}{h^2}\left(\frac{\partial S_x^P}{\partial x} + \frac{\partial S_y^P}{\partial y}\right)\right]$$

$$+ \frac{\partial w_0}{\partial x} L_{1,5} w_0 + \frac{\partial w_0}{\partial y} L_{2,5} w_0 + \frac{\partial}{\partial x}\left(N_x \frac{\partial w_0}{\partial x} + N_{xy}\frac{\partial w_0}{\partial y}\right) + \frac{\partial}{\partial y}\left(N_x \frac{\partial w_0}{\partial x} + N_{xy}\frac{\partial w_0}{\partial y}\right)$$

$$= \left[-I_0 \ddot{w}_0 + \left(\frac{4}{3h^2}\right)^2 I_6 \frac{\partial^2}{\partial t^2}\left(\frac{\partial^2 w_0}{\partial x^2} + \frac{\partial^2 w_0}{\partial y^2}\right) - \frac{4}{3h^2} I_3 \frac{\partial^3}{\partial t^2}\left(\frac{\partial u_0}{\partial t} + \frac{\partial v_0}{\partial t}\right)\right.$$

$$\left. - \frac{4}{3h^2}\bar{I}_4 \frac{\partial^2}{\partial t^2}\left(\frac{\partial \phi_x}{\partial x} + \frac{\partial \phi_y}{\partial y}\right)\right] \tag{1e}$$

with the following pre-loaded boundary conditions.

Along the edges $x = a_1,\ a_2$

$$N_x \text{ or } u_0; \quad N_{xy} \text{ or } v_0; \quad M_x - \frac{4}{3h^2}T_x \text{ or } \phi_x; \quad M_{xy} - \frac{4}{3h^2}T_{xy} \text{ or } \phi_y;$$

$$T_x \text{ or } \frac{\partial w_0}{\partial x}; \quad \left(N_x \frac{\partial w_0}{\partial x} + N_{xy}\frac{\partial w_0}{\partial y} + Q_x - \frac{4}{3h^2}\frac{\partial T_{xy}}{\partial y} + \frac{4}{h^2}S_x\right) \text{ or } w_0;$$

and along the edges $y = b_1,\ b_2$

$$N_{xy} \text{ or } u_0; \quad N_y \text{ or } v_0; \quad M_{xy} - \frac{4}{3h^2}T_{xy} \text{ or } \phi_x; \quad M_y - \frac{4}{3h^2}T_y \text{ or } \phi_y;$$

$$T_y \text{ or } \frac{\partial w_0}{\partial y}; \quad \left(N_{xy} \frac{\partial w_0}{\partial x} + N_y\frac{\partial w_0}{\partial y} + Q_y - \frac{4}{3h^2}\frac{\partial T_{xy}}{\partial x} + \frac{4}{h^2}S_y\right) \text{ or } w_0.$$

It is explicitly indicated that the above governing equation set is a high-order coupled nonlinear differential equation system, including five variables to be determined, and each boundary edge has six pre-loaded boundary conditions. Therefore, it is almost impossible for someone to use analytical solutions to work it out except some special cases. Then, the numerical methods become the quite considerable solution tools to solve the coupled nonlinear differential equations system (Bellman and Casti, 1971; Villadsen and Michelsen, 1978; Bert and Malik, 1996; Malik and Bert, 1996; Bellomo, 1997; Shu, 2000). Due to the reason of large-deflection effect and existence of the overlapping boundary conditions for the present solving problem, we have to abandon the common FEM method and here develop a new differential quadrature method, called as Hermite differential quadrature (HDQ) method, to solve the highly coupled nonlinear differential equations with the prescribed overlapping boundary conditions.

As is well known, any function $f(x)$ can be approximated by an interpolation function $\psi(x)$ with a set of undetermined weighted coefficients $W_i(x)$ at an increscent discrete point set $\{x_1, x_2, \ldots, x_N\}$, such as Lagrange interpolation, Chebyshev interpolation, as follows:

$$f(x) \approx \psi(x) = \sum_{i=1}^{N} W_i(x) f_i, \tag{2}$$

where f_i is the point value of function $f(x)$ at the ith point.

The basic idea of differential quadrature (DQ) method can be originated from the ordinary differential equation. Similar to differential theorem, the rth order derivation of the unknown function $f(x)$ at any discrete points can be obtained by the rth order derivative of the interpolation function, namely, a weighted linear sum of the function values at all the discrete points $\{x_1, x_2, \ldots x_N\}$,

$$f^{(r)}(x) = \frac{\partial^r f(x)}{\partial x^r} = \frac{\partial^r \psi(x)}{\partial x^r} = \sum_{i=1}^{N} \frac{\partial^r W_i(x)}{\partial x^r} f_i \quad (i = 1, 2, \ldots, N) \tag{3a}$$

and at the jth point

$$f^{(r)}(x_j) = \left.\frac{\partial^r f(x)}{\partial x^r}\right|_{x=x_j} = \sum_{i=1}^{N} \frac{\partial^r W_i(x_j)}{\partial x^r} f_i = \sum_{i=1}^{N} A_{ij}^{(r)} f_i \quad (j = 1, 2, \ldots, n), \tag{3b}$$

where the superscript r in the bracket denotes the rth order derivative. $A_{ij}^{(r)}$ are the weighted coefficients for the rth order derivative at the point x_i of DQ method. For a common Lagrangian interpolation theorem always used in DQM, the weighted coefficients $W_i(x)$ in Eq. (3) can be presented by

$$W_i(x) = l_i(x) = \frac{P_n(x)}{(x - x_i) P_n^{(1)}(x_i)} \quad (i = 1, 2, \ldots, N), \tag{4}$$

where $P_n(x)$ is a polynomial and $P_n(x) = (x - x_1)(x - x_2)\cdots(x - x_N)$. $P_n^{(1)}(x)$ is the first-order derivative of $P_n(x)$. It is obvious that the weighted coefficients have the delta function characteristics. Further, the kth order derivative of the weighted coefficients $W_i(x)$ for the Lagrange interpolation can be obtained by

$$l_i^{(k-1)}(x_i) = \frac{1}{k} \frac{P_n^{(k)}(x_i)}{P_n^{(1)}(x_i)} \quad \text{for } x = x_i \text{ and } k = 1, \ldots, n \tag{5a}$$

and

$$l_i^{(k)}(x_j) = \frac{1}{x_j - x_i} \left[\frac{P_n^{(k)}(x_j)}{P_n^{(1)}(x_i)} - k l_i^{(k-1)}(x_j) \right] \quad \text{for } x = x_j \neq x_i \text{ and } k = 1, \ldots, n. \tag{5b}$$

Thus, the weighted coefficients $A_{ij}^{(r)}$ can be obtained

$$A_{ij}^{(k)} = l_i^{(k)}(x_j). \tag{6}$$

For a two-dimensional case, the above weighted coefficient construction method can be extended to construct the weighted coefficients in a 2-D case as follows:

$$f(x, y_j) = \sum_{i=1}^{N} l_i(x) f(x_i, y_j) \quad (j = 1, 2, \ldots, M), \tag{7a}$$

$$f(x_i, y) = \sum_{i=1}^{M} g_j(y) f(x_i, y_j) \quad (i = 1, 2, \ldots, N) \tag{7b}$$

and further

$$f(x, y) = \sum_{i=1}^{N} \sum_{j=1}^{M} l_i(x) g_j(y) f(x_i, y_j), \tag{7c}$$

where $g_j(y)$ is the Lagrangian interpolation along the y-direction and constructed in a same process as $l_i(x)$. Similarly for the kth order derivative of $g_j(y)$, we also have

$$B_{ij}^{(k)} = g_j^{(k)}(y_i). \tag{8}$$

The above formulation derivation is a general formula constructing procedure for the common differential quadrature (DQ) method. Although the DQ method has been verified as a much effective numerical method to solve the differential equations, it is hard to implement the overlapping boundary condition problems in the engineering, such as Bernoulli–Euler beam and classical plate etc. Therefore, we here based on the Hermite interpolation theorem to develop a new generalized differential quadrature method, called as generalized Hermite differential quadrature (HDQ) method, which much considers the exact approximation up to the first-order differential of unknown function at an interpolated point. As is well known, the general expression of Hermite interpolation theorem for an unknown function in a set of discretization points $\{x_1 < x_2 < \cdots < x_N\}$ in one-dimensional case can be presented by

$$\phi(x) = \sum_{i=1}^{N} h_i(x) f(x_i) + \sum_{i=1}^{R} \bar{h}_i(x) f^{(1)}(x_i) = \sum_{i=1}^{N+R} H_i(x) F_i, \tag{9}$$

where N is the total discrete point number in an interpolation domain. R is the number of those interpolated points where the interpolation function and its first-order differential are required to be equal to the point-values of the unknown function and its first-order differential respectively, and, $1 \leqslant R \leqslant N$. Here, $[F_i] = \{f_1, f_2, \ldots, f_n, f_1^{(1)}, f_2^{(1)}, \ldots, f_r^{(1)}\}$ and $[H_i] = \{h_1(x), \ldots, h_N(x), \bar{h}_1(x), \ldots, \bar{h}_R(x)\}$. $h_i(x)$ and $\bar{h}_i(x)$ are the weighted functions of the interpolation function and its first-order differential of the interpolation function in the ith point respectively. It is very noted that the weighted functions $h_i(x)$ and $\bar{h}_i(x)$ must have the following characteristics based on Hermite interpolation theory:

$$h_i(x_j) = \delta_{ij} \quad (i, j = 1, 2, \ldots, N); \qquad h_i^{(1)}(x_j) = 0 \quad (i = 1, 2, \ldots, N;\ j = 1, 2, \ldots, R), \tag{10a}$$

$$\bar{h}_i(x_j) = 0 \quad (i = 1, 2, \ldots, R;\ j = 1, 2, \ldots, N); \qquad \bar{h}_i^{(1)}(x_j) = 0 \quad (i, j = 1, 2, \ldots, R). \tag{10b}$$

And, the generalized Hermite differential quadrature can be further obtained for the kth order differential as follows:

$$f^{(k)}(x) = \frac{\partial^k f(x)}{\partial x^k} = \sum_{i=1}^{N+R} \frac{\partial^k H_i(x)}{\partial x^k} F_i \quad (i = 1, 2, \ldots, N). \tag{11}$$

In order to determine the weighted functions, we can assume the following general expressions of $h_i(x)$ and $\bar{h}_i(x)$ to satisfy the above four equations (i.e., Eq. (10)):

$$h_i(x) = \begin{cases} t_i(x) l_{\mathrm{in}}(x) l_{\mathrm{ir}}(x), & i = 1, 2, \ldots, R, \\ l_{\mathrm{in}}(x) \frac{P_r(x)}{P_r(x_i)}, & i = R+1, R+2, \ldots, N \end{cases} \tag{12a}$$

and

$$\bar{h}_i(x) = s_i(x - x_i)l_{\rm in}(x)l_{\rm ir}(x), \quad i = 1, 2, \ldots, R, \tag{12b}$$

where $t_i(x)$ is a polynomial to be determined and s_i an unknown constant. Clearly, $h_i(x) \in H_{n+r}$ and $\bar{h}_i(x) \in M_{n+r}$. Here, $P_r(x) = (x - x_1)(x - x_2)\cdots(x - x_r)$ and $l_{\rm in}$ is the Lagrangian interpolation for the total scattered points' set N and $l_{\rm ir}$ is the Lagrangian interpolation for the partial scattered points' set R.

Substitution of the above assumed solutions, i.e. Eq. (12), into the requirement Eq. (10) can obtain the unknown polynomial $t_i(x)$ and constant s_i

$$t_i(x) = 1 - (x - x_i)[l_{\rm in}^{(1)}(x_i) + l_{\rm ir}^{(1)}(x_i)] \quad \text{and} \quad s_i = 1 \ \ (i = 1, 2, \ldots, R). \tag{13}$$

Up to now, the general equations of Hermite interpolation function $\phi(x)$ for the unknown function $f(x)$ are completely set up. Here, some extreme cases can be carried out as follows:

While $r = 0$, the interpolation function can be reduced to the general Lagrange interpolation function.

While $r = n$, the weighted functions in Eq. (12) become

$$h_i(x) = [1 - 2(x - x_i)l_{\rm in}^{(1)}(x_i)][l_{\rm in}(x)]^2, \quad i = 1, 2, \ldots, N, \tag{14a}$$

$$\bar{h}_i(x) = (x - x_i)[l_{\rm in}(x)]^2. \tag{14b}$$

Clearly, this result was known as Hermite's interpolation formula (Hermite, 1878).

In this paper, we cared more about how to solve the boundary value differential equations with the overlapping boundary conditions, such as the Bernoulli–Euler beam and classical plate etc. For most of overlapping boundary condition problems, it is clear that R is equal to 2, i.e. the two boundary points x_1 and x_N. Thus, only substituting x_1 and x_N into Eqs. (12) and (13), we can easily and directly obtain the detailed weighted function of HDQ method written as follows:

$$\bar{h}_1(x) = (x - x_1)l_{1n}(x)\frac{x - x_N}{x_1 - x_N} = l_{1n}(x)\frac{x^2 - (x_1 + x_N)x + x_1x_N}{x_1 - x_N}, \tag{15a}$$

$$\bar{h}_n(x) = (x - x_N)l_{1n}(x)\frac{x - x_1}{x_N - x_1} = l_{1n}(x)\frac{x^2 - (x_1 + x_N)x + x_1x_N}{x_N - x_1}, \tag{15b}$$

$$h_1(x) = \left[1 - (x - x_1)\left(l_{1n}^{(1)}(x_1) + \frac{1}{x_1 - x_N}\right)\right]l_{1n}(x)\frac{x - x_1}{x_1 - x_N}, \tag{15c}$$

$$h_n(x) = \left[1 - (x - x_N)\left(l_{nn}^{(1)}(x_N) + \frac{1}{x_N - x_1}\right)\right]l_{1n}(x)\frac{x - x_N}{x_N - x_1}, \tag{15d}$$

$$h_j(x) = \frac{(x - x_1)(x - x_N)}{(x_j - x_1)(x_j - x_N)}l_{jn}(x), \quad j = 2, 3, \ldots, N - 1. \tag{15e}$$

Exactly, these results are same to the expressions of the generalized differential quadrature method developed by Liu and Wu (2001a,b). It is noted that our developed Hermite differential quadrature method is more simple and convenient to obtain the weighted functions than Liu and Wu's GDQ method, especially for those cases of $i > 2$. In the case of $i > 2$, we can directly obtain the weighted functions by using Eqs. (12) and (13) but Liu and Wu's GDQ method need re-construct the interpolation functions based on the Hermite interpolation characteristics, about which the detailed advantages and discussion can be referred to Cheng (in press).

For a two-dimensional case, the Hermite interpolation $\phi(x,y)$ of present HDQ method for the unknown function can be presented in a same manner as the differential quadrature method as

$$\phi(x,y)=\sum_{i=1}^{N_x}\sum_{j=1}^{N_y}h_i(x)h_j(y)f(x_i,y_j)+\sum_{j=1}^{N_y}\sum_{i=1}^{R_x}l_j(y)\bar{h}_i(x)f^{(1x)}(x_i,y_j)+\sum_{i=1}^{N_x}\sum_{j=1}^{R_y}l_i(x)\bar{h}_j(x)f^{(1y)}(x_i,y_j). \tag{16}$$

Based on the above constructed Hermite differential quadrature interpolation, the generalized Hermite differential quadrature expressions for the mth order x-derivatives at any point (x_i, y_j) can be written as follows:

$$\frac{\partial^m\phi(x_i,y_j)}{\partial x^m}=\sum_{k=1}^{N_x+R_x}H_{ik}^{(m)}F_{kj},\quad i=1,2,\ldots,N_x,\ \ j=1,2,\ldots,N_y. \tag{17}$$

In a same manner, the generalized Hermite differential quadrature expression for the nth order x-derivatives at any point (x_i, y_j) can be obtained

$$\frac{\partial^n\phi(x_i,y_j)}{\partial y^n}=\sum_{l=1}^{N_y+R_y}L_{jl}^{(n)}F_{il},\quad i=1,2,\ldots,N_x,\ \ j=1,2,\ldots,N_y, \tag{18}$$

where $L_{jl}^{(n)}$ is the weighted coefficient for the scattered points along y-direction and can be constructed in a same process to $H_{ik}^{(n)}$.

Similarly, the generalized Hermite differential quadrature expression for a mix derivative has the following form:

$$\frac{\partial^{(m+n)}\phi(x_i,y_j)}{\partial x^m\,\partial y^n}=\sum_{k=1}^{N_x}\sum_{l=1}^{N_y}H_{ik}^{(m)}L_{jl}^{(n)}F_{kl}+\sum_{l=1}^{N_y}\sum_{k=n_x+1}^{N_x+R_x}B_{jl}^{(n)}H_{ik}^{(m)}F_{kl}+\sum_{k=1}^{N_x}\sum_{l=n_y+1}^{N_y+R_y}A_{ik}^{(m)}L_{jl}^{(n)}F_{kl},$$
$$i=1,2,\ldots,N_x,\ \ j=1,2,\ldots,N_y, \tag{19}$$

where the weighted coefficients A and B are defined in Eqs. (6) and (8).

3. Application and discretization

In this section, the presently developed theory model for anisotropic piezoelectric/composite plate and numerical HDQ method are employed to study and verify the electro-elastic behavior of a typical three-layer sandwich anisotropic plate contained with the piezoelectric core layer which has a spatially distributed poling direction, as shown in Fig. 2 of Part I. While the distributed poling angle $\alpha_p = 0$ and $\beta_p = 0$, the extension-twisting coupling of anisotropic piezoelectric/composite plate was developed to be the driven element in the rotary motor by Lee et al. (1998). Here, we make this rotary motor element as an example, i.e. anti-symmetrical laminated fiber reinforced composite plate with a PZT-5H plate core. Thus, it is clear that the following general stiffness components of the anti-symmetrical piezoelectric/composite laminate are zero:

$A_{16} = A_{26} = B_{11} = B_{12} = B_{66} = F_{11} = F_{12} = F_{66} = D_{16} = D_{26} = H_{16} = H_{26} = J_{16} = J_{26} = 0$ and $A_{45} = D_{45} = H_{45} = 0$.

Then, the static governing equations for the anti-symmetrical piezoelectric/composite laminated plate can be simplified from the Eq. (1) as follows:

$$
\begin{aligned}
&A_{11}\frac{\partial^2 u_0}{\partial x^2}+A_{66}\frac{\partial^2 u_0}{\partial y^2}+G_3\frac{\partial^2 v_0}{\partial x\,\partial y}+2G_1\frac{\partial^2 \phi_x}{\partial x\,\partial y}+G_1\frac{\partial^2 \phi_y}{\partial x^2}+G_2\frac{\partial^2 \phi_y}{\partial y^2}-\frac{4}{3h^2}\left(3F_{16}\frac{\partial^3 w_0}{\partial x^2\,\partial y}+F_{26}\frac{\partial^3 w_0}{\partial y^3}\right)\\
&\quad\underline{+\frac{\partial w_0}{\partial x}\left(A_{11}\frac{\partial^2 w_0}{\partial x^2}+A_{66}\frac{\partial^2 w_0}{\partial y^2}\right)+(A_{12}+A_{66})\frac{\partial w_0}{\partial y}\frac{\partial^2 w_0}{\partial x\,\partial y}}=\frac{\partial N_x^p}{\partial x}+\frac{\partial N_{xy}^p}{\partial x},
\end{aligned}
\tag{20a}
$$

$$
\begin{aligned}
&G_3\frac{\partial^2 u_0}{\partial x\,\partial y}+A_{66}\frac{\partial^2 v_0}{\partial x^2}+A_{22}\frac{\partial^2 v_0}{\partial y^2}+G_1\frac{\partial^2 \phi_x}{\partial x^2}+G_2\frac{\partial^2 \phi_x}{\partial y^2}+2G_2\frac{\partial^2 \phi_y}{\partial x\,\partial y}-\frac{4}{3h^2}\left(F_{16}\frac{\partial^3 w_0}{\partial x^3}+3F_{26}\frac{\partial^3 w_0}{\partial x\,\partial y^2}\right)\\
&\quad\underline{+(A_{12}+A_{66})\frac{\partial w}{\partial x}\frac{\partial^2 w}{\partial x\,\partial y}+\frac{\partial w_0}{\partial y}\left(A_{66}\frac{\partial^2 w}{\partial x^2}+A_{22}\frac{\partial^2 w}{\partial y^2}\right)}=\frac{\partial N_y^p}{\partial y}+\frac{\partial N_{xy}^p}{\partial y},
\end{aligned}
\tag{20b}
$$

$$
\begin{aligned}
&2G_1\frac{\partial^2 u_0}{\partial x\,\partial y}+G_1\frac{\partial^2 v_0}{\partial x^2}+G_2\frac{\partial^2 v_0}{\partial y^2}+G_7\frac{\partial^2 \phi_x}{\partial x^2}+G_8\frac{\partial^2 \phi_x}{\partial y^2}-G_5\phi_x+G_{12}\frac{\partial^2 \phi_y}{\partial x\,\partial y}-G_5\frac{\partial w_0}{\partial x}-G_{10}\frac{\partial^3 w_0}{\partial x^3}\\
&\quad-G_{13}\frac{\partial^3 w_0}{\partial x\,\partial y^2}\underline{+\left(B_{16}-\frac{4}{3h^2}F_{16}\right)\left(2\frac{\partial w_0}{\partial x}\frac{\partial^2 w_0}{\partial x\,\partial y}+\frac{\partial w_0}{\partial y}\frac{\partial^2 w_0}{\partial x^2}\right)+\left(B_{26}-\frac{4}{3h^2}F_{26}\right)\frac{\partial w_0}{\partial x}\frac{\partial^2 w_0}{\partial y^2}}\\
&\quad=\left[\frac{\partial M_x^P}{\partial x}+\frac{\partial M_{xy}^P}{\partial y}-Q_x^P+\frac{4}{h^2}S_x^P-\frac{4}{3h^2}\left(\frac{\partial T_x^P}{\partial x}+\frac{\partial T_{xy}^P}{\partial y}\right)\right],
\end{aligned}
\tag{20c}
$$

$$
\begin{aligned}
&G_1\frac{\partial^2 u_0}{\partial x^2}+G_2\frac{\partial^2 u_0}{\partial y^2}+2G_2\frac{\partial^2 v_0}{\partial x\,\partial y}+G_{12}\frac{\partial^2 \phi_x}{\partial x\,\partial y}+G_8\frac{\partial^2 \phi_y}{\partial x^2}+G_9\frac{\partial^2 \phi_y}{\partial y^2}-G_4\phi_y-G_4\frac{\partial w_0}{\partial y}-G_{13}\frac{\partial^3 w_0}{\partial x^2\,\partial y}\\
&\quad-G_{11}\frac{\partial^3 w_0}{\partial y^3}\underline{+\left(B_{16}-\frac{4}{3h^2}F_{16}\right)\frac{\partial w_0}{\partial x}\frac{\partial^2 w_0}{\partial x^2}+\left(B_{26}-\frac{4}{3h^2}F_{26}\right)\left(\frac{\partial w_0}{\partial x}\frac{\partial^2 w_0}{\partial y^2}+2\frac{\partial w_0}{\partial y}\frac{\partial^2 w_0}{\partial x\,\partial y}\right)}\\
&\quad=\left[\frac{\partial M_y^P}{\partial y}+\frac{\partial M_{xy}^P}{\partial x}-Q_y^P+\frac{4}{h^2}S_y^P-\frac{4}{3h^2}\left(\frac{\partial T_y^P}{\partial y}+\frac{\partial T_{xy}^P}{\partial x}\right)\right],
\end{aligned}
\tag{20d}
$$

$$
\begin{aligned}
&-\frac{4}{3h^2}\left(3F_{16}\frac{\partial^3 u_0}{\partial x^2\,\partial y}+F_{26}\frac{\partial^3 u_0}{\partial y^3}\right)-\frac{4}{3h^2}\left(F_{16}\frac{\partial^3 v_0}{\partial x^3}+3F_{26}\frac{\partial^3 v_0}{\partial x\,\partial y^2}\right)-G_5\frac{\partial \phi_x}{\partial x}-G_{10}\frac{\partial^3 \phi_x}{\partial x^3}-G_{13}\frac{\partial^3 \phi_x}{\partial x\,\partial y^2}\\
&\quad-G_4\frac{\partial \phi_y}{\partial y}-G_{13}\frac{\partial^3 \phi_y}{\partial x^2\,\partial y}-G_{11}\frac{\partial^3 \phi_y}{\partial y^3}-(G_5-N_{x0})\frac{\partial^2 w_0}{\partial x^2}-G_4\frac{\partial^2 w_0}{\partial y^2}+\frac{16}{9h^4}\left[J_{11}\frac{\partial^4 w_0}{\partial x^4}+2(J_{12}+2J_{66})\frac{\partial^4 w_0}{\partial x^2\,\partial y^2}\right.\\
&\quad\left.+J_{22}\frac{\partial^4 w_0}{\partial y^4}\right]\underline{-\frac{4}{3h^2}\frac{\partial w_0}{\partial x}\left(3F_{16}\frac{\partial^3 w_0}{\partial x^2\,\partial y}+F_{26}\frac{\partial^3 w_0}{\partial y^3}\right)-\frac{4}{3h^2}\frac{\partial w_0}{\partial y}\left(F_{16}\frac{\partial^3 w_0}{\partial x^3}+3F_{26}\frac{\partial^3 w_0}{\partial x\,\partial y^2}\right)}\\
&\quad=\left[\frac{\partial Q_x^P}{\partial x}+\frac{\partial Q_y^P}{\partial y}-\frac{4}{3h^2}\left(\frac{\partial^2 T_x^P}{\partial x^2}+\frac{\partial^2 T_{xy}^P}{\partial x\,\partial y}+\frac{4}{3h^2}\frac{\partial^2 T_y^P}{\partial y^2}\right)+\frac{4}{h^2}\left(\frac{\partial S_x^P}{\partial x}+\frac{\partial S_y^P}{\partial y}\right)\right]
\end{aligned}
\tag{20e}
$$

and the relevant stress resultants and moments can be also presented by the mid-plane displacement functions as

$$N_1 = A_{11}\left(\frac{\partial u_0}{\partial x} + \underline{\frac{1}{2}\left(\frac{\partial w_0}{\partial x}\right)^2}\right) + A_{12}\left(\frac{\partial v_0}{\partial y} + \underline{\frac{1}{2}\left(\frac{\partial w_0}{\partial y}\right)^2}\right) + B_{16}\left(\frac{\partial \phi_x}{\partial y} + \frac{\partial \phi_y}{\partial x}\right) - \frac{4}{3h^2}F_{16}\left(\frac{\partial \phi_y}{\partial x} + \frac{\partial \phi_x}{\partial y} + 2\frac{\partial^2 w_0}{\partial y \partial x}\right) - N_x^p,$$

$$N_2 = A_{12}\left(\frac{\partial u_0}{\partial x} + \underline{\frac{1}{2}\left(\frac{\partial w_0}{\partial x}\right)^2}\right) + A_{22}\left(\frac{\partial v_0}{\partial y} + \underline{\frac{1}{2}\left(\frac{\partial w_0}{\partial y}\right)^2}\right) + B_{26}\left(\frac{\partial \phi_x}{\partial y} + \frac{\partial \phi_y}{\partial x}\right) - \frac{4}{3h^2}F_{26}\left(\frac{\partial \phi_y}{\partial x} + \frac{\partial \phi_x}{\partial y} + 2\frac{\partial^2 w_0}{\partial y \partial x}\right) - N_y^p,$$

$$N_{12} = A_{66}\left(\frac{\partial u_0}{\partial y} + \frac{\partial v_0}{\partial x} + \underline{\frac{\partial w_0}{\partial x}\frac{\partial w_0}{\partial y}}\right) + B_{16}\frac{\partial \phi_x}{\partial x} + B_{26}\frac{\partial \phi_y}{\partial y} - \frac{4}{3h^2}F_{16}\left(\frac{\partial^2 w_0}{\partial x^2} + \frac{\partial \phi_x}{\partial x}\right) - \frac{4}{3h^2}F_{26}\left(\frac{\partial \phi_y}{\partial y} + \frac{\partial^2 w_0}{\partial y^2}\right) - N_{xy}^p,$$

$$M_1 = B_{16}\left(\frac{\partial u_0}{\partial y} + \frac{\partial v_0}{\partial x} + \underline{\frac{\partial w_0}{\partial x}\frac{\partial w_0}{\partial y}}\right) + D_{11}\frac{\partial \phi_x}{\partial x} + D_{12}\frac{\partial \phi_y}{\partial y} - \frac{4}{3h^2}H_{11}\left(\frac{\partial^2 w_0}{\partial x^2} + \frac{\partial \phi_x}{\partial x}\right) - \frac{4}{3h^2}H_{12}\left(\frac{\partial \phi_y}{\partial y} + \frac{\partial^2 w_0}{\partial y^2}\right) - M_1^p,$$

$$M_2 = B_{26}\left(\frac{\partial u_0}{\partial y} + \frac{\partial v_0}{\partial x} + \underline{\frac{\partial w_0}{\partial x}\frac{\partial w_0}{\partial y}}\right) + D_{12}\frac{\partial \phi_x}{\partial x} + D_{22}\frac{\partial \phi_y}{\partial y} - \frac{4}{3h^2}H_{12}\left(\frac{\partial^2 w_0}{\partial x^2} + \frac{\partial \phi_x}{\partial x}\right) - \frac{4}{3h^2}H_{22}\left(\frac{\partial \phi_y}{\partial y} + \frac{\partial^2 w_0}{\partial y^2}\right) - M_2^p,$$

$$M_{12} = B_{16}\left(\frac{\partial u_0}{\partial x} + \underline{\frac{1}{2}\left(\frac{\partial w_0}{\partial x}\right)^2}\right) + B_{26}\left(\frac{\partial v_0}{\partial y} + \underline{\frac{1}{2}\left(\frac{\partial w_0}{\partial y}\right)^2}\right) + D_{66}\left(\frac{\partial \phi_x}{\partial y} + \frac{\partial \phi_y}{\partial x}\right) - \frac{4}{3h^2}H_{66}\left(\frac{\partial \phi_y}{\partial x} + \frac{\partial \phi_x}{\partial y} + 2\frac{\partial^2 w_0}{\partial y \partial x}\right) - M_{12}^p,$$

$$T_1 = F_{16}\left(\frac{\partial u_0}{\partial y} + \frac{\partial v_0}{\partial x} + \underline{\frac{\partial w_0}{\partial x}\frac{\partial w_0}{\partial y}}\right) + H_{11}\frac{\partial \phi_x}{\partial x} + H_{12}\frac{\partial \phi_y}{\partial y} - \frac{4}{3h^2}J_{11}\left(\frac{\partial^2 w_0}{\partial x^2} + \frac{\partial \phi_x}{\partial x}\right) - \frac{4}{3h^2}J_{12}\left(\frac{\partial \phi_y}{\partial y} + \frac{\partial^2 w_0}{\partial y^2}\right) - T_1^p,$$

$$T_2 = F_{26}\left(\frac{\partial u_0}{\partial y} + \frac{\partial v_0}{\partial x} + \underline{\frac{\partial w_0}{\partial x}\frac{\partial w_0}{\partial y}}\right) + H_{12}\frac{\partial \phi_x}{\partial x} + H_{22}\frac{\partial \phi_y}{\partial y} - \frac{4}{3h^2}J_{12}\left(\frac{\partial^2 w_0}{\partial x^2} + \frac{\partial \phi_x}{\partial x}\right) - \frac{4}{3h^2}J_{22}\left(\frac{\partial \phi_y}{\partial y} + \frac{\partial^2 w_0}{\partial y^2}\right) - T_2^p,$$

$$T_{12} = F_{16}\left(\frac{\partial u_0}{\partial x} + \underline{\frac{1}{2}\left(\frac{\partial w_0}{\partial x}\right)^2}\right) + F_{26}\left(\frac{\partial v_0}{\partial y} + \underline{\frac{1}{2}\left(\frac{\partial w_0}{\partial y}\right)^2}\right) + H_{66}\left(\frac{\partial \phi_x}{\partial y} + \frac{\partial \phi_y}{\partial x}\right) - \frac{4}{3h^2}J_{66}\left(\frac{\partial \phi_y}{\partial x} + \frac{\partial \phi_x}{\partial y} + 2\frac{\partial^2 w_0}{\partial y \partial x}\right) - T_{12}^p,$$

where the underline terms are related to the large-deflection effect terms.

From the above mentioned boundary conditions, it is found that only the boundary conditions about W are overlapping boundary conditions. Then, based on the developed generalized Hermite differential quadrature method, we only set $R = 2$ to construct the interpolation function for the unknown function w_0 otherwise use $R = 0$ to form the interpolation functions for other unknown functions u_0, v_0, ϕ_x and ϕ_y, and then substitute them into governing equations to obtain the discrete equations in any interior point (x_i, y_j)

$$\begin{aligned}
&A_{11}\sum_{k=1}^{n_x} A_{ik}^{(2)} u_{0kj} + A_{66}\sum_{l=1}^{n_y} B_{jl}^{(2)} u_{0il} + G_3\sum_{k=1}^{n_x}\sum_{l=1}^{n_y} A_{ik}^{(1)} B_{jl}^{(1)} v_{0kl} + 2G_1\sum_{k=1}^{n_x}\sum_{l=1}^{n_y} A_{ik}^{(1)} B_{jl}^{(1)} \phi_{xkl} + G_1\sum_{k=1}^{n_x} A_{ik}^{(2)}\phi_{ykj} \\
&\quad + G_2\sum_{l=1}^{n_y} B_{jl}^{(2)}\phi_{yil} - \frac{4}{3h^2}\left[3F_{16}\left(\sum_{k=1}^{n_x}\sum_{l=1}^{n_y} H_{ik}^{(2)} L_{jl}^{(1)} W_{kl} + \sum_{l=1}^{n_y}\sum_{k=n_x+1}^{n_x+r_x} B_{jl}^{(1)} H_{ik}^{(2)} W_{kl} + \sum_{k=1}^{n_x}\sum_{l=n_y+1}^{n_y+r_y} A_{ik}^{(2)} L_{jl}^{(1)} W_{kl}\right)\right. \\
&\quad \left. + F_{26}\sum_{l=1}^{n_y+r_y} L_{jl}^{(3)} W_{il}\right] + \underline{\sum_{k=1}^{n_x+r_x} H_{ik}^{(1')} W_{kj}\left(A_{11}\sum_{k=1}^{n_x+r_x} H_{ik}^{(2')} W_{kj} + A_{66}\sum_{l=1}^{n_y+r_y} L_{jl}^{(2)} W_{il}\right) + (A_{12}+A_{66})} \\
&\quad \underline{\sum_{l=1}^{n_y+r_y} L_{jl}^{(1)} W_{il}\left(\sum_{k=1}^{n_x}\sum_{l=1}^{n_y} H_{ik}^{(1)} L_{jl}^{(1)} W_{kl} + \sum_{l=1}^{n_y}\sum_{k=n_x+1}^{n_x+r_x} B_{jl}^{(1)} H_{ik}^{(1)} W_{kl} + \sum_{k=1}^{n_x}\sum_{l=n_y+1}^{n_y+r_y} A_{ik}^{(1)} L_{jl}^{(1)} W_{kl}\right)} = \left.\frac{\partial N_x^p}{\partial x}\right|_{ij} + \left.\frac{\partial N_{xy}^p}{\partial y}\right|_{ij},
\end{aligned} \tag{21a}$$

$$
\begin{aligned}
&G_3 \sum_{k=1}^{n_x}\sum_{l=1}^{n_y} A_{ik}^{(1)} B_{jl}^{(1)} u_{0kl} + A_{66}\sum_{k=1}^{n_x} A_{ik}^{(2)} v_{0kj} + A_{22}\sum_{l=1}^{n_y} B_{jl}^{(2)} v_{0il} + G_1 \sum_{k=1}^{n_x} A_{ik}^{(2)}\phi_{xkj} + G_2\sum_{l=1}^{n_y} B_{jl}^{(2)}\phi_{xil}\\
&+ 2G_2 \sum_{k=1}^{n_x}\sum_{l=1}^{n_y} A_{ik}^{(1)} B_{jl}^{(1)}\phi_{ykl} - \frac{4}{3h^2}\Bigg[F_{16}\sum_{k=1}^{n_x+r_x} H_{ik}^{(3)}W_{kj} + 3F_{26}\Bigg(\sum_{k=1}^{n_x}\sum_{l=1}^{n_y} H^{(1)}_{ik}L^{(2)}_{jl}W_{kl} + \sum_{k=1}^{n_x}\sum_{l=1}^{r_y} A^{(1)}_{ik}L^{(2)}_{jl}W_{kl}\\
&+ \sum_{k=1}^{r_x}\sum_{l=1}^{n_y} B^{(2)}_{jl}H^{(1)}_{ik}W_{kl}\Bigg)\Bigg] + \underline{(A_{12}+A_{66})\sum_{k=1}^{n_x+r_x} H^{(1)}_{ik}W_{kj}\Bigg(\sum_{k=1}^{n_x}\sum_{l=1}^{n_y} H^{(1)}_{ik}L^{(2)}_{jl}W_{kl} + \sum_{k=1}^{n_x}\sum_{l=n_y+1}^{n_y+r_y} A^{(1)}_{ik}L^{(2)}_{jl}W_{kl}}\\
&\underline{+\sum_{k=n_x+1}^{n_x+r_x}\sum_{l=1}^{n_y}B^{(2)}_{jl}H^{(1)}_{ik}W_{kl}}\Bigg) + \sum_{l=1}^{n_y+r_y} L^{(1)}_{jl}W_{il}\Bigg(A_{66}\sum_{k=1}^{n_x+r_x}H^{(2)}_{ik}W_{kj} + A_{22}\sum_{l=1}^{n_y+r_y}L^{(2)}_{jl}W_{il}\Bigg) = \left.\frac{\partial N_y^p}{\partial y}\right|_{ij} + \left.\frac{\partial N^p_{xy}}{\partial x}\right|_{ij},
\end{aligned}
\tag{21b}
$$

$$
\begin{aligned}
&2G_1 \sum_{k=1}^{n_x}\sum_{l=1}^{n_y} A_{ik}^{(1)} B_{jl}^{(1)} u_{0kl} + G_1\sum_{k=1}^{n_x} A_{ik}^{(2)} v_{0kj} + G_2\sum_{l=1}^{n_y} B_{jl}^{(2)} v_{0il} + G_7 \sum_{k=1}^{n_x} A_{ik}^{(2)}\phi_{xkj} + G_8\sum_{l=1}^{n_y} B_{jl}^{(2)}\phi_{xil} - G_5\phi_{xij}\\
&+ G_{12} \sum_{k=1}^{n_x}\sum_{l=1}^{n_y} A_{ik}^{(1)} B_{jl}^{(1)}\phi_{ykl} - G_5\sum_{k=1}^{n_x} H^{(1)}_{ik}W_{kj} - G_{10}\sum_{k=1}^{n_x+r_x} H^{(3)}_{ik}W_{kj} - G_{13}\Bigg(\sum_{k=1}^{n_x}\sum_{l=1}^{n_y} H^{(1)}_{ik}L^{(2)}_{jl}W_{kl}\\
&+\sum_{k=1}^{n_x}\sum_{l=n_y+1}^{n_y+r_y} A^{(1)}_{ik}L^{(2)}_{jl}W_{kl} + \sum_{k=n_x+1}^{n_x+r_x}\sum_{l=1}^{n_y} B^{(2)}_{jl}H^{(1)}_{ik}W_{kl}\Bigg) + \underline{\left(B_{16}-\frac{4}{3h^2}F_{16}\right)\Bigg[2\sum_{k=1}^{n_x+r_x} H^{(1)}_{ik}W_{kj}\Bigg(\sum_{k=1}^{n_x}\sum_{l=1}^{n_y} H^{(1)}_{ik}L^{(1)}_{jl}W_{kl}}\\
&\underline{+\sum_{k=1}^{n_x}\sum_{l=n_y+1}^{n_y+r_y} A^{(1)}_{ik}L^{(1)}_{jl}W_{kl} + \sum_{k=n_x+1}^{n_x+r_x}\sum_{l=1}^{n_y} B^{(2)}_{jl}H^{(1)}_{ik}W_{kl}\Bigg) + \sum_{l=1}^{n_y+r_y} L^{(1)}_{jl}W_{il}\sum_{k=1}^{n_x+r_x} H^{(2)}_{ik}W_{kj}\Bigg] + \left(B_{26}-\frac{4}{3h^2}F_{26}\right)}\\
&\underline{\times\sum_{k=1}^{n_x+r_x} H^{(1)}_{ik}W_{kj}\sum_{l=1}^{n_y+r_y} L^{(2)}_{jl}W_{il}} = \left[\left.\frac{\partial M_x^P}{\partial x}\right|_{ij} + \left.\frac{\partial M_{xy}^P}{\partial y}\right|_{ij} - Q_x^P|_{ij} + \left.\frac{4}{h^2}S_x^P\right|_{ij} - \frac{4}{3h^2}\left(\left.\frac{\partial T_x^P}{\partial x}\right|_{ij} + \left.\frac{\partial T_{xy}^P}{\partial y}\right|_{ij}\right)\right],
\end{aligned}
\tag{21c}
$$

$$
\begin{aligned}
&G_1 \sum_{k=1}^{n_x} A_{ik}^{(2)} u_{0lj} + G_2\sum_{l=1}^{n_y} B_{jl}^{(2)} u_{0il} + 2G_2\sum_{k=1}^{n_x}\sum_{l=1}^{n_y} A_{ik}^{(1)} B_{jl}^{(1)} v_{0kl} + G_{12}\sum_{k=1}^{n_x}\sum_{l=1}^{n_y} A_{ik}^{(1)} B_{jl}^{(1)}\phi_{xkl} + G_8\sum_{k=1}^{n_x} A_{ik}^{(2)}\phi_{ykj}\\
&+ G_9\sum_{l=1}^{n_y} B_{jl}^{(2)}\phi_{yil} - G_4\phi_{yij} - G_4\sum_{l=1}^{n_y+r_y} L^{(1)}_{jl}W_{il} - G_{13}\Bigg(\sum_{k=1}^{n_x}\sum_{l=1}^{n_y} H^{(2)}_{ik}L^{(1)}_{jl}W_{kl} + \sum_{l=1}^{n_y}\sum_{k=n_x+1}^{n_x+r_x} B^{(1)}_{jl}H^{(2)}_{ik}W_{kl}\\
&+\sum_{k=1}^{n_x}\sum_{l=n_y+1}^{n_y+r_y} A^{(2)}_{ik}L^{(1)}_{jl}W_{kl}\Bigg) - G_{11}\sum_{l=1}^{n_y+r_y} L^{(3)}_{jl}W_{il} + \underline{\left(B_{16}-\frac{4}{3h^2}F_{16}\right)\sum_{k=1}^{n_x+r_x} H^{(1')}_{ik}W_{kj}\sum_{k=1}^{n_x+r_x} H^{(2')}_{ik}W_{kj} + \left(B_{26}-\frac{4}{3h^2}F_{26}\right)}\\
&\underline{\times\Bigg[\sum_{k=1}^{n_x+r_x} H^{(1)}_{ik}W_{kj}\sum_{l=1}^{n_y+r_y} L^{(1)}_{jl}W_{il} + 2\sum_{l=1}^{n_y+r_y} L^{(1)}_{jl}W_{il}\Bigg(\sum_{k=1}^{n_x}\sum_{l=1}^{n_y} H^{(1)}_{ik}L^{(1)}_{jl}W_{kl} + \sum_{l=1}^{n_y}\sum_{k=n_x+1}^{n_x+r_x} B^{(1)}_{jl}H^{(1)}_{ik}W_{kl} + \sum_{k=1}^{n_x}\sum_{l=n_y+1}^{n_y+r_y} A^{(1)}_{ik}L^{(1)}_{jl}W_{kl}\Bigg)\Bigg]}\\
&= \left[\left.\frac{\partial M_y^P}{\partial y}\right|_{ij} + \left.\frac{\partial M_{xy}^P}{\partial x}\right|_{ij} - Q_y^P|_{ij} + \frac{4}{h^2}S_y^P|_{ij} - \frac{4}{3h^2}\left(\left.\frac{\partial T_y^P}{\partial y}\right|_{ij} + \left.\frac{\partial T_{xy}^P}{\partial x}\right|_{ij}\right)\right],
\end{aligned}
\tag{21d}
$$

$$
\begin{aligned}
&-\frac{4}{3h^2}\left(3F_{16}\sum_{k=1}^{n_x}\sum_{l=1}^{n_y}A_{ik}^{(2)}B_{jl}^{(1)}u_{0kl}+F_{26}\sum_{l=1}^{n_y}B_{jl}^{(3)}u_{0il}\right)-\frac{4}{3h^2}\left(F_{16}\sum_{k=1}^{n_x}A_{ik}^{(3)}v_{0kj}+3F_{26}\sum_{k=1}^{n_x}\sum_{l=1}^{n_y}A_{ik}^{(1)}B_{jl}^{(2)}v_{0kl}\right)\\
&-G_5\sum_{k=1}^{n_x}A_{ik}^{(1)}\phi_{xkj}-G_{10}\sum_{k=1}^{n_x}A_{ik}^{(3)}\phi_{xkj}-G_{13}\sum_{k=1}^{n_x}\sum_{l=1}^{n_y}A_{ik}^{(1)}B_{jl}^{(2)}\phi_{xkl}-G_4\sum_{l=1}^{n_y}B_{jl}^{(1)}\phi_{yil}-G_{13}\sum_{k=1}^{n_x}\sum_{l=1}^{n_y}A_{ik}^{(2)}B_{jl}^{(1)}\phi_{ykl}\\
&-G_{11}\sum_{l=1}^{n_y}B_{jl}^{(3)}\phi_{yil}-(G_5-N_{x0})\sum_{i=1}^{n_x+r_x}H_{ik}^{(2)}W_{kj}-G_4\sum_{l=1}^{n_y+r_y}L_{jl}^{(2)}W_{il}+\frac{16}{9h^4}\left[J_{11}\sum_{i=1}^{n_x+r_x}H_{ik}^{(4)}W_{kj}+2(J_{12}+2J_{66})\right.\\
&\left.\times\left(\sum_{k=1}^{n_x}\sum_{l=1}^{n_y}H_{ik}^{(2)}L_{jl}^{(2)}W_{kl}+\sum_{k=1}^{n_x}\sum_{l=n_y+1}^{n_y+r_y}A_{ik}^{(2)}L_{jl}^{(2)}W_{kl}+\sum_{k=n_x+1}^{n_x+r_x}\sum_{l=1}^{n_y}B_{jl}^{(2)}H_{ik}^{(2)}W_{kl}\right)+J_{22}\sum_{l=1}^{n_y+r_y}L_{jl}^{(4)}W_{il}\right]\\
&\underline{-\frac{4}{3h^2}\sum_{k=1}^{n_x+r_x}H_{ik}^{(1)}W_{kj}\left[3F_{16}\left(\sum_{k=1}^{n_x}\sum_{l=1}^{n_y}H_{ik}^{(2)}L_{jl}^{(1)}W_{kl}+\sum_{k=1}^{n_x}\sum_{l=n_y+1}^{n_y+r_y}A_{ik}^{(2)}L_{jl}^{(1)}W_{kl}+\sum_{k=n_x+1}^{n_x+r_x}\sum_{l=1}^{n_y}B_{jl}^{(1)}H_{ik}^{(2)}W_{kl}\right)\right.}\\
&\underline{\left.+F_{26}\sum_{l=1}^{n_y+r_y}L_{jl}^{(3)}W_{il}\right]}-\underline{\frac{4}{3h^2}\sum_{l=1}^{n_y+r_y}L_{jl}^{(1)}W_{il}\left[F_{16}\sum_{k=1}^{n_x+r_x}H_{ik}^{(3)}W_{kj}+3F_{26}\left(\sum_{k=1}^{n_x}\sum_{l=1}^{n_y}H_{ik}^{(1)}L_{jl}^{(2)}W_{kl}+\sum_{k=1}^{n_x}\sum_{l=n_y+1}^{n_y+r_y}A_{ik}^{(1)}L_{jl}^{(2)}W_{kl}\right.\right.}\\
&\underline{\left.\left.+\sum_{k=n_x+1}^{n_x+r_x}\sum\nolimits_{l=1}^{n_y}B_{jl}^{(2)}H_{ik}^{(1)}W_{kl}\right)\right]}=\left[\left.\frac{\partial Q_x^P}{\partial x}\right|_{ij}+\left.\frac{\partial Q_y^P}{\partial y}\right|_{ij}-\frac{4}{3h^2}\left(\left.\frac{\partial^2 T_x^P}{\partial x^2}\right|_{ij}+\left.\frac{\partial^2 T_{xy}^P}{\partial x\,\partial y}\right|_{ij}+\frac{4}{3h^2}\left.\frac{\partial^2 T_y^P}{\partial y^2}\right|_{ij}\right)\right.\\
&\left.+\frac{4}{h^2}\left(\left.\frac{\partial S_x^P}{\partial x}\right|_{ij}+\left.\frac{\partial S_y^P}{\partial y}\right|_{ij}\right)\right].
\end{aligned}
\tag{21e}
$$

Similarly, the force resultants can be also discretized by the interpolation functions as follows:

$$
\begin{aligned}
N_1|_{ij}=&A_{11}\left(\sum_{k=1}^{n_x}A_{ik}^{(1)}u_{0kj}+\underline{\frac{1}{2}\left(\sum_{k=1}^{n_x+r_x}H_{ik}^{(1)}W_{kj}\right)^2}\right)+A_{12}\left(\sum_{l=1}^{n_y}B_{jl}^{(1)}v_{0il}+\underline{\frac{1}{2}\left(\sum_{l=1}^{n_y+r_y}B_{jl}^{(1)}W_{il}\right)^2}\right)\\
&+B_{16}\left(\sum_{l=1}^{n_y}B_{jl}^{(1)}\phi_{xil}+\sum_{k=1}^{n_x}A_{ik}^{(1)}\phi_{ykj}\right)-\frac{4}{3h^2}F_{16}\left[\sum_{l=1}^{n_y}B_{jl}^{(1)}\phi_{xil}+\sum_{k=1}^{n_x}A_{ik}^{(1)}\phi_{ykj}\right.\\
&\left.+2\left(\sum_{k=1}^{n_x}\sum_{l=1}^{n_y}H_{ik}^{(1)}L_{jl}^{(1)}W_{kl}+\sum_{k=1}^{n_x}\sum_{l=n_y+1}^{r_y+n_y}A_{ik}^{(1)}L_{jl}^{(1)}W_{kl}+\sum_{k=n_x+1}^{n_x+r_x}\sum_{l=1}^{n_y}B_{jl}^{(1)}H_{ik}^{(1)}W_{kl}\right)\right]-N_x^p|_{ij},
\end{aligned}
\tag{a}
$$

$$
\begin{aligned}
N_2|_{ij}=&A_{12}\left(\sum_{k=1}^{n_x}A_{ik}^{(1)}u_{0kj}+\underline{\frac{1}{2}\left(\sum_{k=1}^{n_x+r_x}H_{ik}^{(1)}W_{kj}\right)^2}\right)+A_{22}\left(\sum_{l=1}^{n_y}B_{jl}^{(1)}v_{0il}+\underline{\frac{1}{2}\left(\sum_{l=1}^{n_y+r_y}B_{jl}^{(1)}W_{il}\right)^2}\right)\\
&+B_{26}\left(\sum_{l=1}^{n_y}B_{jl}^{(1)}\phi_{xil}+\sum_{k=1}^{n_x}A_{ik}^{(1)}\phi_{ykj}\right)-\frac{4}{3h^2}F_{26}\left[\sum_{l=1}^{n_y}B_{jl}^{(1)}\phi_{xil}+\sum_{k=1}^{n_x}A_{ik}^{(1)}\phi_{ykj}+2\left(\sum_{k=1}^{n_x}\sum_{l=1}^{n_y}H_{ik}^{(1)}L_{jl}^{(1)}W_{kl}\right.\right.\\
&\left.\left.+\sum_{k=1}^{n_x}\sum_{l=n_y+1}^{r_y+n_y}A_{ik}^{(1)}L_{jl}^{(1)}W_{kl}+\sum_{k=n_x+1}^{n_x+r_x}\sum_{l=1}^{n_y}B_{jl}^{(1)}H_{ik}^{(1)}W_{kl}\right)\right]-N_x^p|_{ij},
\end{aligned}
\tag{b}
$$

$$
\begin{aligned}
N_{12}|_{ij} = {} & A_{66}\left(\sum_{l=1}^{n_y} B_{jl}^{(1)} u_{0il} + \sum_{k=1}^{n_x} A_{ik}^{(1)} v_{0kj} \underline{+ \sum_{k=1}^{n_x+r_x} H_{ik}^{(1)} W_{kj} \sum_{l=1}^{n_y+r_y} L_{jl}^{(1)} W_{il}}\right) + B_{16}\sum_{k=1}^{n_x} A_{ik}^{(1)} \phi_{xkj} + B_{26} \\
& \times \sum_{l=1}^{n_y} B_{jl}^{(1)} \phi_{yil} - \frac{4}{3h^2} F_{16}\left(\sum_{k=1}^{n_x+r_x} H_{ik}^{(2)} W_{kj} + \sum_{k=1}^{n_x} A_{ik}^{(1)} \phi_{xkj}\right) \\
& - \frac{4}{3h^2} F_{26}\left(\sum_{l=1}^{n_y} B_{jl}^{(1)} \phi_{yil} + \sum_{l=1}^{n_y+r_y} L_{jl}^{(2)} W_{il}\right) - N_{xy}^{p}|_{ij},
\end{aligned}
\tag{c}
$$

$$
\begin{aligned}
M_{1}|_{ij} = {} & B_{16}\left(\sum_{l=1}^{n_y} B_{jl}^{(1)} u_{0il} + \sum_{k=1}^{n_x} A_{ik}^{(1)} v_{0kj} \underline{+ \sum_{k=1}^{n_x+r_x} H_{ik}^{(1)} W_{kj} \sum_{l=1}^{n_y+r_y} L_{jl}^{(1)} W_{il}}\right) + D_{11}\sum_{k=1}^{n_x} A_{ik}^{(1)} \phi_{xkj} + D_{12} \\
& \times \sum_{l=1}^{n_y} B_{jl}^{(1)} \phi_{yil} - \frac{4}{3h^2} H_{11}\left(\sum_{k=1}^{n_x+r_x} H_{ik}^{(2)} W_{kj} + \sum_{k=1}^{n_x} A_{ik}^{(1)} \phi_{xkj}\right) \\
& - \frac{4}{3h^2} H_{12}\left(\sum_{l=1}^{n_y} B_{jl}^{(1)} \phi_{yil} + \sum_{l=1}^{n_y+r_y} L_{jl}^{(2)} W_{il}\right) - M_{x}^{p}|_{ij},
\end{aligned}
\tag{d}
$$

$$
\begin{aligned}
M_{2}|_{ij} = {} & B_{26}\left(\sum_{l=1}^{n_y} B_{jl}^{(1)} u_{0il} + \sum_{k=1}^{n_x} A_{ik}^{(1)} v_{0kj} \underline{+ \sum_{k=1}^{n_x+r_x} H_{ik}^{(1)} W_{kj} \sum_{l=1}^{n_y+r_y} L_{jl}^{(1)} W_{il}}\right) + D_{12}\sum_{k=1}^{n_x} A_{ik}^{(1)} \phi_{xkj} \\
& + D_{22}\sum_{l=1}^{n_y} B_{jl}^{(1)} \phi_{yil} - \frac{4}{3h^2} H_{12}\left(\sum_{k=1}^{n_x+r_x} H_{ik}^{(2)} W_{kj} + \sum_{k=1}^{n_x} A_{ik}^{(1)} \phi_{xkj}\right) \\
& - \frac{4}{3h^2} H_{22}\left(\sum_{l=1}^{n_y} B_{jl}^{(1)} \phi_{yil} + \sum_{l=1}^{n_y+r_y} L_{jl}^{(2)} W_{il}\right) - M_{y}^{p}|_{ij},
\end{aligned}
\tag{e}
$$

$$
\begin{aligned}
M_{12}|_{ij} = {} & B_{16}\left(\sum_{k=1}^{n_x} A_{ik}^{(1)} u_{0kj} \underline{+ \frac{1}{2}\left(\sum_{k=1}^{n_x+r_x} H_{ik}^{(1)} W_{kj}\right)^2}\right) + B_{26}\left(\sum_{l=1}^{n_y} B_{jl}^{(1)} v_{0il} \underline{+ \frac{1}{2}\left(\sum_{l=1}^{n_y+r_y} B_{jl}^{(1)} W_{il}\right)^2}\right) \\
& + D_{66}\left(\sum_{l=1}^{n_y} B_{jl}^{(1)} \phi_{xil} + \sum_{k=1}^{n_x} A_{ik}^{(1)} \phi_{ykj}\right) - \frac{4}{3h^2} H_{66}\left[\sum_{l=1}^{n_y} B_{jl}^{(1)} \phi_{xil} + \sum_{k=1}^{n_x} A_{ik}^{(1)} \phi_{ykj}\right. \\
& \left. + 2\left(\sum_{k=1}^{n_x}\sum_{l=1}^{n_y} H_{ik}^{(1)} L_{jl}^{(1)} W_{kl} + \sum_{k=1}^{n_x}\sum_{l=n_y+1}^{r_y+n_y} A_{ik}^{(1)} L_{jl}^{(1)} W_{kl} + \sum_{k=n_x+1}^{n_x+r_x}\sum_{l=1}^{n_y} B_{jl}^{(1)} H_{ik}^{(1)} W_{kl}\right)\right] - M_{xy}^{p}|_{ij},
\end{aligned}
\tag{f}
$$

$$
\begin{aligned}
T_{1}|_{ij} = {} & F_{16}\left(\sum_{l=1}^{n_y} B_{jl}^{(1)} u_{0il} + \sum_{k=1}^{n_x} A_{ik}^{(1)} v_{0kj} \underline{+ \sum_{k=1}^{n_x+r_x} H_{ik}^{(1)} W_{kj} \sum_{l=1}^{n_y+r_y} L_{jl}^{(1)} W_{il}}\right) + H_{11}\sum_{k=1}^{n_x} A_{ik}^{(1)} \phi_{xkj} + H_{12} \\
& \times \sum_{l=1}^{n_y} B_{jl}^{(1)} \phi_{yil} - \frac{4}{3h^2} J_{11}\left(\sum_{k=1}^{n_x+r_x} H_{ik}^{(2)} W_{kj} + \sum_{k=1}^{n_x} A_{ik}^{(1)} \phi_{xkj}\right) \\
& - \frac{4}{3h^2} J_{12}\left(\sum_{l=1}^{n_y} B_{jl}^{(1)} \phi_{yil} + \sum_{l=1}^{n_y+r_y} L_{jl}^{(2)} W_{il}\right) - T_{x}^{p}|_{ij},
\end{aligned}
\tag{g}
$$

$$T_2|_{ij} = F_{26}\left(\sum_{l=1}^{n_y} B_{jl}^{(1)} u_{0il} + \sum_{k=1}^{n_x} A_{ik}^{(1)} v_{0kj} + \underline{\sum_{k=1}^{n_x+r_x} H_{ik}^{(1)} W_{kj} \sum_{l=1}^{n_y+r_y} L_{jl}^{(1)} W_{il}}\right) + H_{12} \sum_{k=1}^{n_x} A_{ik}^{(1)} \phi_{xkj} + H_{22}$$
$$\times \sum_{l=1}^{n_y} B_{jl}^{(1)} \phi_{yil} - \frac{4}{3h^2} J_{12}\left(\sum_{k=1}^{n_x+r_x} H_{ik}^{(2)} W_{kj} + \sum_{k=1}^{n_x} A_{ik}^{(1)} \phi_{xkj}\right)$$
$$- \frac{4}{3h^2} J_{22}\left(\sum_{l=1}^{n_y} B_{jl}^{(1)} \phi_{yil} + \sum_{l=1}^{n_y+r_y} L_{jl}^{(2)} W_{il}\right) - T_y^p|_{ij}, \tag{h}$$

$$T_{12}|_{ij} = F_{16}\left(\sum_{k=1}^{n_x} A_{ik}^{(1)} u_{0kj} + \underline{\frac{1}{2}\left(\sum_{k=1}^{n_x+r_x} H_{ik}^{(1)} W_{kj}\right)^2}\right) + F_{26}\left(\sum_{l=1}^{n_y} B_{jl}^{(1)} v_{0il} + \underline{\frac{1}{2}\left(\sum_{l=1}^{n_y+r_y} B_{jl}^{(1)} W_{il}\right)^2}\right)$$
$$+ H_{66}\left(\sum_{l=1}^{n_y} B_{jl}^{(1)} \phi_{xil} + \sum_{k=1}^{n_x} A_{ik}^{(1)} \phi_{ykj}\right) - \frac{4}{3h^2} J_{66}\left[\sum_{l=1}^{n_y} B_{jl}^{(1)} \phi_{xil} + \sum_{k=1}^{n_x} A_{ik}^{(1)} \phi_{ykj}\right.$$
$$\left. + 2\left(\sum_{k=1}^{n_x} \sum_{l=1}^{n_y} H_{ik}^{(1)} L_{jl}^{(1)} W_{kl} + \sum_{k=1}^{n_x} \sum_{l=n_y+1}^{r_y+n_y} A_{ik}^{(1)} L_{jl}^{(1)} W_{kl} + \sum_{k=n_x+1}^{n_x+r_x} \sum_{l=1}^{n_y} B_{jl}^{(1)} H_{ik}^{(1)} W_{kl}\right)\right] - T_{xy}^p|_{ij}. \tag{i}$$

The clamped boundary condition along x-axis must be satisfied as follows:

$$w_0 = u_0 = v_0 = \phi_x = \phi_y = \frac{\partial w_0}{\partial x} = 0. \tag{22a}$$

The free condition along x-axis must be satisfied as follows:

$$N_x = N_{xy} = M_x - \frac{4}{3h^2} T_x = T_x = M_{xy} - \frac{4}{3h^2} T_{xy} = N_x \frac{\partial w_0}{\partial x} + N_{xy} \frac{\partial w_0}{\partial y} + Q_x - \frac{4}{3h} \frac{\partial T_{xy}}{\partial y} + \frac{4}{h^2} S_x$$
$$= 0. \tag{22b}$$

The simply-supported boundary condition along x-axis must be satisfied as follows:

$$w_0 = N_{xy} = M_x - \frac{4}{3h^2} T_x = T_x = M_{xy} - \frac{4}{3h^2} T_{xy} = N_x \frac{\partial w_0}{\partial x} + N_{xy} \frac{\partial w_0}{\partial y} + Q_x - \frac{4}{3h} \frac{\partial T_{xy}}{\partial y} + \frac{4}{h^2} S_x = 0. \tag{22c}$$

Along y-axis, the similar overlapping boundary conditions can be obtained in terms of the relative boundary conditions of Part I. Then, using the constructed interpolations and the discretized force resultants, we can also obtain the relevant discretization boundary conditions for the prescribed boundary conditions. Here, the point values of the applied electric field induced resultant forces and moments are also directly obtained in the scattered points with the following difference and integration:

$$\frac{\partial H(x - x_0)}{\partial x} = \delta(x - x_0), \qquad \int f(x)\delta(x - x_0) = f(x_0),$$

which can be further used to describe the partially covered electrode distribution of piezoelectric layer. Now, combining the discrete governing equations and relevant boundary conditions, a complete set of algebraic expressions for the solving problem can be obtained and solved to carry out the final point-values of mid-plane displacements in all the scattered points.

4. Numerical results and discussion

In accordance with the above theoretical analysis model and developed numerical method-HDQ, we can numerically calculate the behavior of PZT-5H/Composite laminated sandwich plate with the different poling direction of PZT layer and different fiber orientation of composite layer by Mathematica Software. Here, the material constants of PZT-5H lamina with the thickness 1 mm and the fiber reinforced epoxy composite lamina with 1 mm are presented in Table 1.

In order to improve the simulation efficiency and accuracy (Shu, 2000), Chebyshev polynomial is significantly utilized to construct the simulation scattered points within the dimensionless simulation domain [0, 1] in this simulation as follows:

$$\bar{x}_i = \frac{1}{2}\left(1 - \cos\frac{i-1}{N_x - 1}\pi\right) \quad \text{and} \quad \bar{y}_i = \frac{1}{2}\left(1 - \cos\frac{i-1}{N_y - 1}\pi\right).$$

Therefore, the above governing equations and relative boundary conditions are respectively transferred into the dimensionless formulations by using $\bar{x} = \frac{x}{a}$ and $\bar{y} = \frac{y}{b}$.

Now, a PZT/composite anti-symmetrically laminated plate with one edge clamped ($x = 0$) and other edges free and poling direction $\alpha_p = 0$, $\beta_p = 0$ of PZT layer is considered as the first validation example. After substituting the relative equations and constructed weighted functions into the governing equations

Table 1
The material properties of composite and piezoelectric lamina

Material	Material coefficients							
	E_1 (GPa)	E_2 (GPa)	G_{12} (GPa)	G_{23} (GPa)	v_{12}	v_{23}	d_{31} (m/V)	d_{33} (m/V)
Composite	138	8.96	7.1		0.3	0.45		
Piezoelectric	61	61	23.3	19.1	0.31	0.31	−274E−12	593E−12

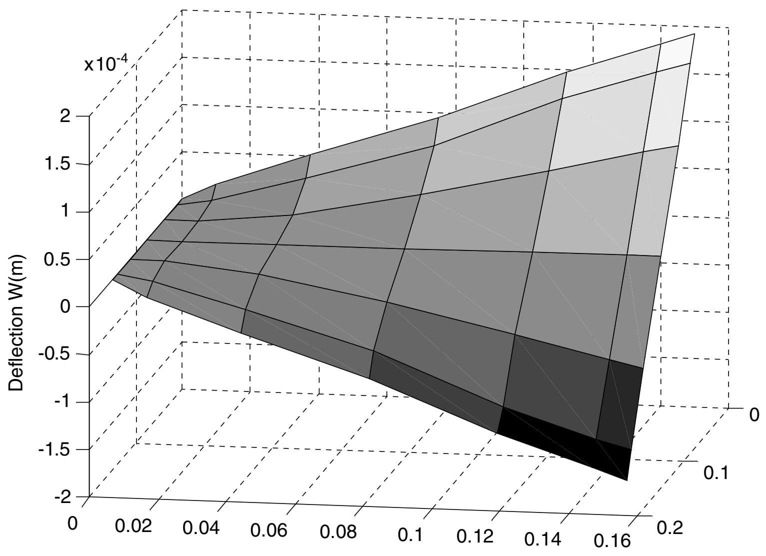

Fig. 1. The deformation shape of PZT/composite anti-symmetrically (±45°) laminated square plate (0.15 m × 0.15 m) with the poling direction α_p, $\alpha_p = 0°$ under the action of electric field $E_3 = 500$ kV/m.

and boundary conditions as shown in Section 3, the final nonlinear discretization algebraic equations about the point-values of mid-plane displacements can be obtained and directly calculated by the Newton's method for all the simulation examples via the Mathematica code. According to the numerical results, the deformation shape of PZT/composite anti-symmetrically laminated plate under the action of electric field is displayed as anti-symmetrical extension-twisting shape as Fig. 1 and the anti-symmetrical maximal deflections always occur along the free edge $x = a$. About the effect of large-amplitude deflections, the nonlinear results in the present analysis are larger than the linear ones as shown in Fig. 2. These comparisons clearly confirmed that the large-amplitude deflection effect must be considered in the theoretical analysis about the PZT/composite laminated plate. Moreover, the effects of the length–width ratio a/b on the deflection along

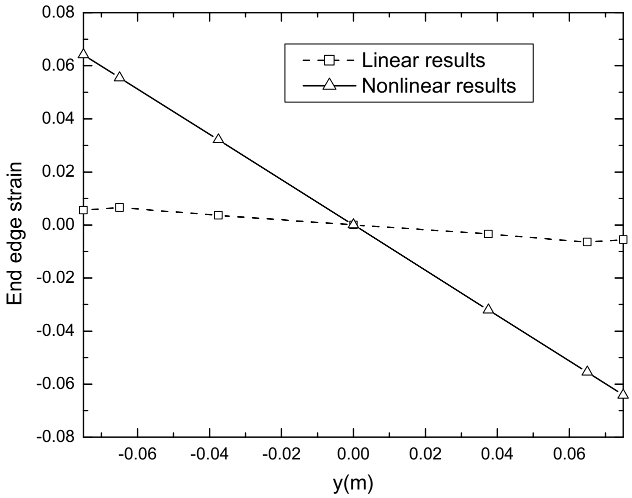

Fig. 2. The comparison between the linear results and nonlinear results to show the nonlinear effect on the end edge strain for a given condition.

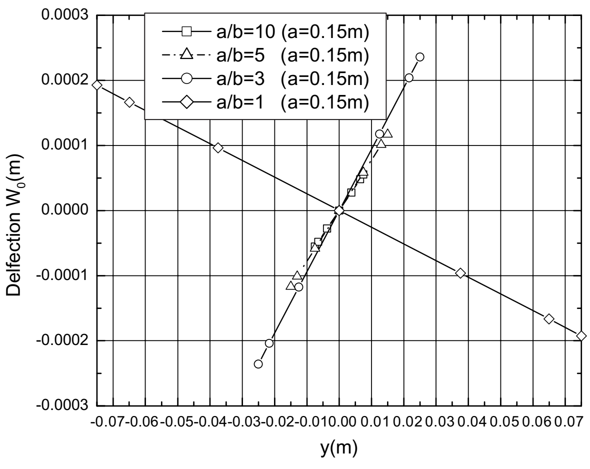

Fig. 3. The detailed effect of the ratio a/b of length and width on the deflection of PZT/composite laminated plate with $\alpha_c \pm 45°$ along the edge $x = a$ at $E_3 = 500$ kV/m.

the free edge ($x = a$) are depicted in Fig. 3 and show that the maximal deflection can be achieved by choosing the suitable ratio a/b. It is obviously found that the maximal deflection of PZT/composite plate with the distributed fiber orientation can be achieved while the ratio a/b is equal to 3. Simultaneously, Fig. 4 presents the effects of length–width ratio a/b on the deflection along the free edge ($y = 0$) and indicates that the y-axial deflections are nonlinear for the different length–width ratio a/b, particularly for $a/b = 3$. For the influence of composite lamina fiber orientation α_c, the numerical results of Fig. 5 reveal the end edge deflections of the anti-symmetric PZT/composite plate can be changed with the fiber orientation and reach the maximal deflection at the fiber orientation $\alpha_c = \pm 60°$ among the simulated cases. It is noted that the

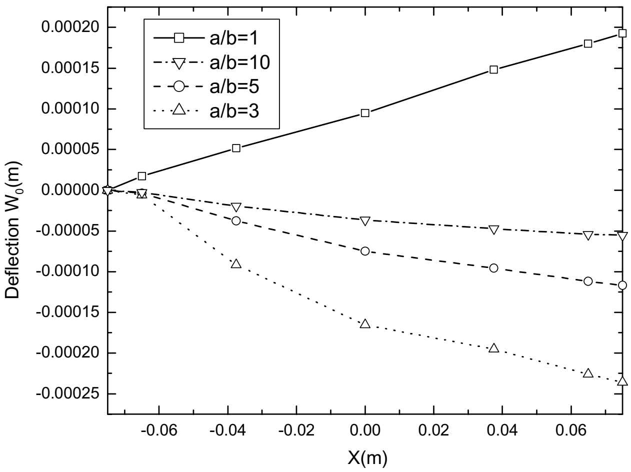

Fig. 4. The detailed effect of the length–width ratio a/b on the deflection of PZT/composite laminated plate with $\alpha_c \pm 45°$ along the edge $y = 0$ at $E_3 = 500$ kV/m.

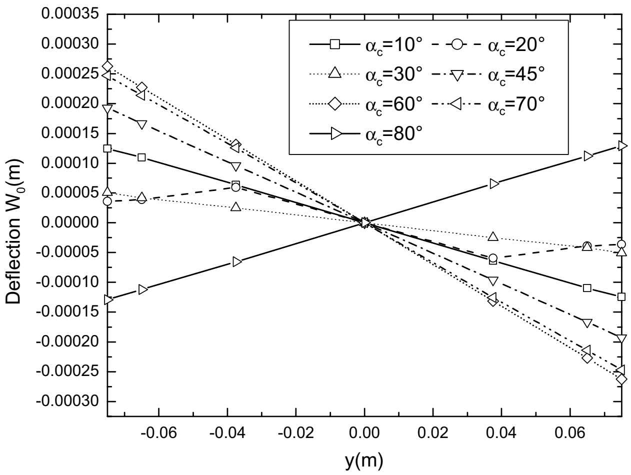

Fig. 5. The effect of the distribution angle of fiber reinforced direction of composite laminate on the end edge deflection along $x = a$ of PZT/composite laminated plate with the ratio $a/b = 1$.

end-edge deflection shape at $\alpha_c = \pm 20°$ is much different from the other fiber orientations. Further, the influences of applied electric field on the deformations of PZT/composite plate with the fiber orientation $\alpha_c = \pm 45°$ and poling direction $\alpha_p = 0$, $\beta_p = 0$ are shown in Figs. 6 and 7. The numerical calculations show that the maximal end-edge deflections can increase nonlinearly with the increment of applied electric field. Moreover, as is well known, the covered electrode area of the PZT core layer is also as a designable factor to take into calculation, as shown in Fig. 8. It is obviously revealed from Fig. 8 that the covered electrode area can play an import role on the plate deformation. And, the numerical simulations show that the maximal deflection of PZT/composite plate can be obtained by only partially covered electrode area in the region $[a/4, a] \times [0, b]$ for a given condition.

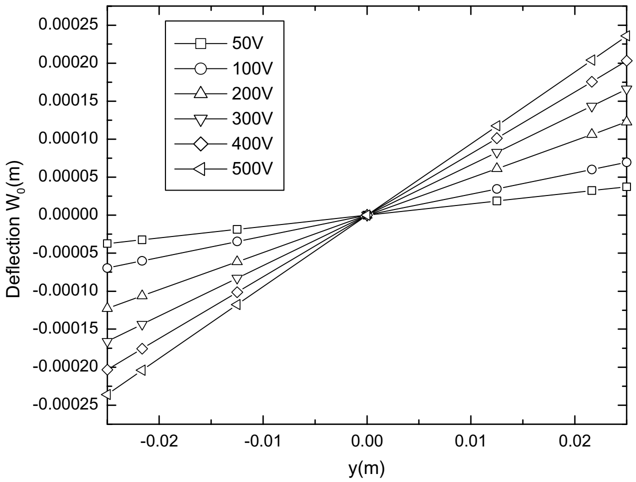

Fig. 6. The influence of the applied electric field on the end edge deflection W_0 of the PZT/composite anti-symmetrically laminated plate with the distribution $\alpha_c = \pm 45°$ and ratio $a/b = 3$.

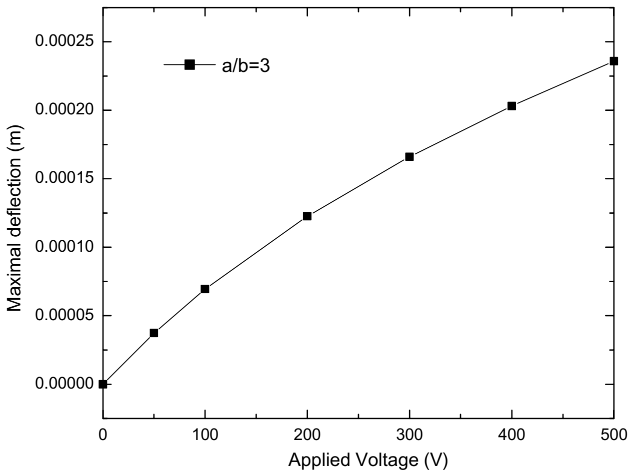

Fig. 7. The effect of the applied electric field on the maximal deflection of PZT/composite anti-symmetrically laminated plate with the distribution angle $\alpha_c = \pm 45°$ and ratio $a/b = 3$.

On the other hand, the effects of the PZT poling direction on the composite plate mechanic behaviors are also investigated in present paper. Fig. 9 shows the deformation of square PZT/composite plate with the fiber orientation $\alpha_c = \pm 45°$ and poling direction $\alpha_p = 90°$ and $\beta_p = 90°$, which is positive nonsymmetrical deflection and different from the plate with the fiber orientation $\alpha_c = \pm 45°$ and poling direction $\alpha_p = 0°$

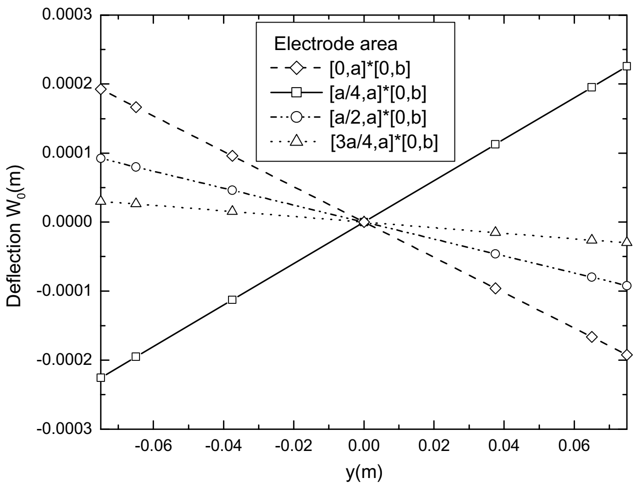

Fig. 8. The effect of the electrode covered area of PZT lay on the edge deflection of PZT/composite laminated plate with the fiber orientation $\alpha_c = \pm 45°$ and ratio $a/b = 3$ at $x = 0$.

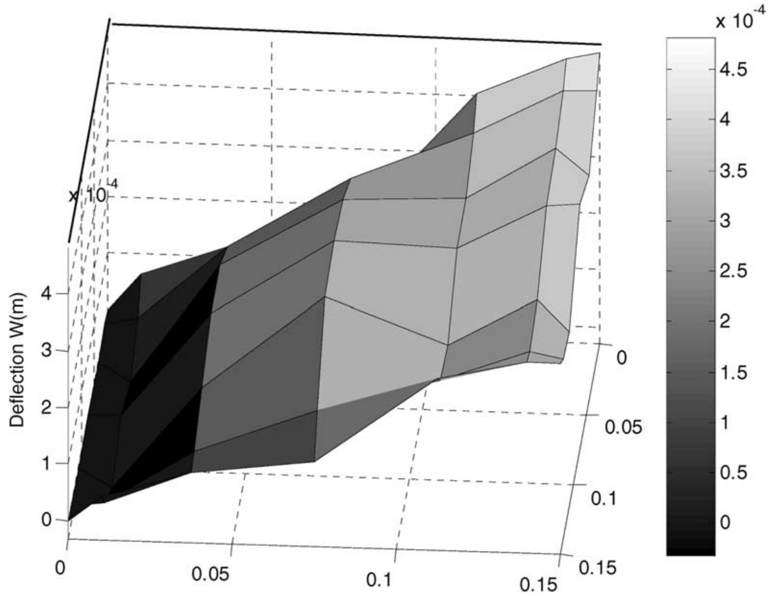

Fig. 9. The deformation shape of PZT/composite anti-symmetrically (±45°) laminated square plate (0.15 m × 0.15 m) with the poling direction α_p, $\beta_p = 90°$ under the action of electric field $E_3 = 500$ kV/m.

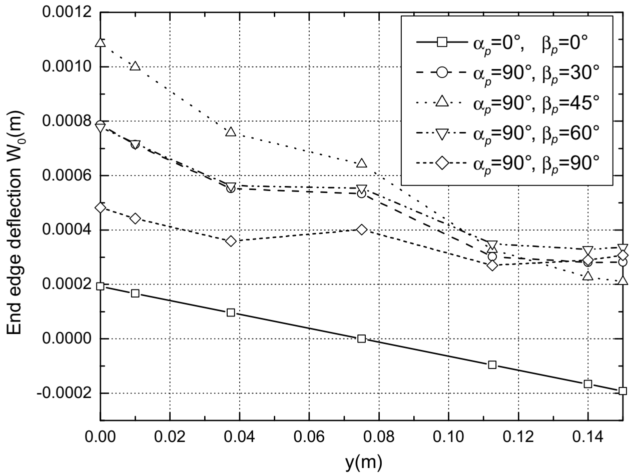

Fig. 10. The influences of the poling direction of PZT lay on the edge deflection of PZT/composite laminated plate with the fiber orientation $\alpha_c = \pm 45°$ and ratio $a/b = 1$ at $x = 0$.

and $\beta_p = 0°$. For the detailed effects of the poling direction on the maximal end-edge deflections, Fig. 10 indicates that the maximal end-edge deflection of the PZT/composite plate can be obtained by integrating the core piezoelectric layer with the poling direction $\alpha_p = 90°$ and $\beta_p = 45°$ under the action of electric field.

From all of the above numerical results, it is explicitly presented that the deformation behavior of PZT/composite laminate plate can be changed through both the fiber orientation of composite material layer and the poling direction and electrode covered area of piezoelectric layer. The maximal deflection of the laminated plate can be accomplished by choosing the suitable factors as investigated in the above numerical studies.

5. Conclusion

Based on Hermite interpolation theory, a new generalized Hermite differential quadrature (HDQ) method was developed to easily implement the overlapping boundary conditions for the high-order coupling differential equations. Then, using the developed generalized HDQ method, the present high-order coupling nonlinear differential equations for the anisotropic piezoelectric/composite plate can be discretized by a set of unknown point-values of mid-plane displacements to form a complete set of algebraic equations system and then solved to work out the final solutions for the point values of mid-plane displacements. Finally, some detailed simulations for smart laminated plate integrated with the piezoelectric plate having a spatial distributed poling direction were studied to validate the developed theory model for piezoelectric/composite plate and numerical method-generalized Hermite differential quadrature method.

Acknowledgement

The authors express their great thanks to the National Natural foundation of China for the excellent Young Investigators.

Appendix A

The stiffness matrix components for the PZT lamina, composite lamina and PZT/composite laminate are shown as following:

$$
\begin{aligned}
G_1 &= B_{16} - \frac{4}{3h^2}F_{16},\\
G_2 &= B_{26} - \frac{4}{3h^2}F_{26},\\
G_3 &= A_{12} + A_{66},\\
G_4 &= A_{44} - \frac{8}{h^2}D_{44} + \frac{16}{h^4}H_{44},\\
G_5 &= A_{55} - \frac{8}{h^2}D_{55} + \frac{16}{h^4}H_{55},\\
G_6 &= A_{45} - \frac{8}{h^2}D_{45} + \frac{16}{h^4}H_{45},\\
G_7 &= D_{11} - \frac{8}{3h^2}H_{11},\\
G_8 &= D_{66} - \frac{8}{3h^2}H_{66} + \frac{16}{9h^4}J_{66},\\
G_9 &= D_{22} - \frac{8}{3h^2}H_{22} + \frac{16}{9h^4}J_{22},\\
G_{10} &= \frac{4}{3h^2}\left(H_{11} - \frac{4}{3h^2}J_{11}\right),\\
G_{11} &= \frac{4}{3h^2}\left(H_{22} - \frac{4}{3h^2}J_{22}\right),\\
G_{12} &= D_{12} + D_{66} - \frac{8}{3h^2}(H_{12} + H_{66}) + \frac{16}{9h^4}(J_{12} + J_{66}),\\
G_{13} &= \frac{4}{3h^2}\left[H_{12} + 2H_{66} - \frac{4}{3h^2}(J_{12} + 2J_{66})\right].
\end{aligned}
$$

References

Bellman, R., Casti, J., 1971. Differential quadrature and long term integration. J. Math. Anal. Appl. 34, 235–238.

Bellomo, N., 1997. Nonlinear models and problems in applied sciences from differential quadrature to generalized collocation methods. Math. Comput. Modell. 26, 13–34.

Bert, C.W., Malik, M., 1996. Differential quadrature method in computational mechanics: A review. Appl. Mech. Rev. 49, 1–27.

Chaudhuri, R.A., 1989. On boundary-discontinuous double Fourier series solution to a system of completely coupled PDEs. Int. J. Eng. Sci. 27 (9), 1005–1022.

Cheng, J.Q., in press. A generalized Hermite differential quadrature approach and its application to elasticity problems with multiple supports.

Cheng, Z.Q., Batra, R.C., 2000. Three-dimensional asymptotic analysis of multiple-electroded piezoelectric laminates. AIAA J. 38, 317–324.

Cheng, J.Q., Qian, C.F., et al., 2000. Effects of electric fields on the bending behavior of PZT-5H piezoelectric laminates. Smart Mater. Struct. 9 (6), 824–831.

Crawley, E., Anderson, E., 1989. Detailed model of piezoelectric actuation of beams. In: Proc. 30th AIAA/ASME/SAE Structure, Structural Dynamics, and Material Conf., Washington, DC, April 1989, pp. 2000–2010.

Donthireddy, P., Chandrasha, K., 1996. Modeling and shape control of composite beams with embedded piezoelectric actuators. Compos. Struct. 35, 237–244.

Fernandes, Pouget, 2002. An accurate modelling of piezoelectric multi-layer plates. Eur. J. Mech. A/Solids 21 (4), 629–651.

Gopinathan, S.V., Varadan, V.V., Varadan, V.K., 2000. A review and critique of theories for piezoeletric laminates. Smart Mater. Struct. 9, 24–48.

Hermite, C., 1878. Sur la Formula d'interpolation de lagrange. J. Reine Angew. Math. 84, 70–79.

Hobson, E.W., 1926. The Theory of Functions of a Real Variable and the Theory of Fourier Series, vol. 11. Cambridge University Press, Cambridge.

Kenji, U., 1998. Piezoelectric ultrasonic motors: Overview. Smart Mater. Struct. 7, 273–285.

Lee, C.K., 1990. Theory of laminated piezoelectric plates for the design of distributed sensors/actuators. Part I: Governing equations and reciprocal relationships. J. Acoust. Soc. Am. 87 (3), 1144–1158.

Lee, S.-W., Ricky, Li, H.L., 1998. Development and characterization of a rotary motor driven by anisotropic piezoelectric composite laminate. Smart Mater. Struct. 7, 327–336.

Liu, G.R., Wu, T.Y., 2001a. Application of generalized differential quadrature rule in Blasius and Onsager equations. Int. J. Numer. Methods Eng. 52 (9), 1013–1027.

Liu, G.R., Wu, T.Y., 2001b. Vibration analysis of beams using the generalized differential quadrature rule and domain decomposition. J. Sound Vib. 246 (3), 461–481.

Liu, G.R., Peng, X.Q., Lam, K.Y., 1999. Vibration control simulation of laminated composite plates with integrated piezoelectrics. J. Sound Vib. 220 (5), 716–735.

Malik, M., Bert, C.W., 1996. Implementing multiple boundary conditions in the DQ solution of higher-order PDEs: Application to free vibration of plates. Int. J. Numer. Methods Eng. 39, 1237–1258.

Pai, P.F., Nayfe, A.H., Oh, K., Mook, D.T., 1993. A refined nonlinear model of composite plates with integrated piezoelectric actuators and sensors. Int. J. Solids Struct. 30 (12), 1603–1630.

Seeley, C.E., Chattopadhyay, A., 1999. Modeling of smart composite laminates including debonding: A finite element approach. Int. J. Solids Struct. 36 (42), 1823–1843.

Shu, C., 2000. Differential Quadrature and Its Application in Engineering. Springer, Great Britain.

Tzou, H.S., Zhong, J.P., 1993. Electromechanics and vibrations of piezoelectric shell distributed systems. J. Dyn. Syst. Measur. Control 115, 506–517.

Villadsen, J., Michelsen, M.L., 1978. Solution of Differential Equation Models by Polynomial by Polynomial Approximation. Prentice-Hall Inc., Englewood Cliffs, NJ.

Whitney, J.M., Leissa, A.W., 1970. Analysis of a simply supported laminated anisotropic rectangular plate. AIAA J. 18, 28–33.

Wu, X.X., Cheng, J.Q., Wang, B., 2001. Influence of applied electric field on the energy release rate for cracked PZT/elastic laminates. Smart Mater. Struct. 10 (5), 970–978.

Zhang, X.D., Sun, C.T., 1996. Formulation of an adaptive sandwich beam. Smart Mater. Struct. 5, 814–823.